Published in final edited form as:
*Neuron*. 2012 March 22; 73(6): 1184–1194. doi:10.1016/j.neuron.2012.02.016.

# Activation of VTA GABA neurons disrupts reward consumption

**Ruud van Zessen**[1,2], **Jana L. Phillips**[1], **Evgeny A. Budygin**[3], and **Garret D. Stuber**[1,*]

[1]Departments of Psychiatry & Cellular and Molecular Physiology, UNC Neuroscience Center, University of North Carolina at Chapel Hill, Chapel Hill, NC 27599, USA [2]Masterprogram Neuroscience and Cognition, Rudolf Magnus Institute, Department of Neuroscience and Pharmacology, University Medical Center Utrecht, Utrecht, 3584 CX, The Netherlands
[3]Department of Physiology and Pharmacology, Wake Forest University School of Medicine, Winston-Salem, NC 27157, USA

## Abstract

The activity of Ventral Tegmental Area (VTA) dopamine (DA) neurons promotes behavioral responses to rewards and environmental stimuli that predict them. VTA GABA inputs synapse directly onto DA neurons and may regulate DA neuronal activity to alter reward-related behaviors, however, the functional consequences of selective activation of VTA GABA neurons remains unknown. Here, we show that *in vivo* optogenetic activation of VTA GABA neurons disrupts reward consummatory behavior, but not conditioned anticipatory behavior in response to reward-predictive cues. In addition, direct activation of VTA GABA projections to the nucleus accumbens (NAc) resulted in detectable GABA release, but did not alter reward consumption. Furthermore, optogenetic stimulation of VTA GABA neurons directly suppressed the activity and excitability of neighboring DA neurons, as well as the release of DA in the NAc, suggesting that the dynamic interplay between VTA DA and GABA neurons can control the initiation and termination of reward-related behaviors.

The Ventral Tegmental Area (VTA) is a heterogeneous brain structure containing neuronal populations that are essential for the expression of motivated behaviors and actions related to addiction and other neuropsychiatric illnesses (Fields et al., 2007; Luscher and Malenka, 2011; Nestler and Carlezon, 2006; Wise, 2004). The VTA contains a mixture of dopaminergic (DA) (~65%), GABAergic (~30%), and glutamatergic neurons (~ 5%) (Margolis et al., 2006; Nair-Roberts et al., 2008; Swanson, 1982; Yamaguchi et al., 2011), that may act in concert to orchestrate reward-seeking behavior. Previous studies have demonstrated that during behavioral conditioning, VTA DA neurons are initially activated by primary rewards, such as sucrose, but following repeated cue-reward pairings shift their activity patterns to predominantly fire to the onset of reward-predictive stimuli (Bromberg-Martin and Hikosaka, 2009; Matsumoto and Hikosaka, 2009; Pan et al., 2005; Tobler et al.,



*Address correspondence to: Garret D. Stuber, Ph.D., Assistant Professor, Departments of Psychiatry & Cell and Molecular Physiology, UNC Neuroscience Center, University of North Carolina at Chapel Hill, Tel: +1 (919) 843-7140, Fax: +1 (919) 966-1050, gstuber@med.unc.edu.

**Author contributions:**
R.v.Z. and G.D.S. conceived and designed all experiments. R.v.Z., J.P., E.A.B., and G.D.S. performed experiments and analyzed the data. R.v.Z. and G.D.S. wrote the manuscript.

2005; Waelti et al., 2001). In addition, exposure to cues that predict natural rewards or drugs of abuse lead to transient surges in dopamine release in the nucleus accumbens (NAc) (Day et al., 2007; Phillips et al., 2003; Roitman et al., 2004; Stuber et al., 2008; Stuber et al., 2005). Furthermore, direct phasic activation of VTA DA neurons can induce behavioral conditioning (Tsai et al., 2009) and facilitate positive reinforcement (Adamantidis et al., 2011) suggesting that dopamine signaling in VTA projection targets such as the NAc may promote the initiation and maintenance of reward-seeking behaviors.

VTA neurons also show distinct firing patterns in response to aversive stimuli. Recordings from putative and identified DA neurons have demonstrated that presentation of aversive stimuli or predictive cues can transiently excite or inhibit DA neuronal activity (Brischoux et al., 2009; Matsumoto and Hikosaka, 2009; Mileykovskiy and Morales, 2011; Mirenowicz and Schultz, 1996; Zweifel et al., 2011). *In vivo*, DA neurons are thought to be tonically inhibited by GABA neurons within the VTA and the Rostromedial Tegmental Nucleus, (Jhou et al., 2009; Johnson and North, 1992b). These midbrain GABA neurons display elevated basal firing rates and a lack of spike accommodation; two electrophysiological characteristics that distinguish them from putative midbrain DA neurons (Steffensen et al., 1998). In addition, VTA GABA neurons increase their firing during cues that predict appetitive rewards (Cohen et al., 2012), and also show a transient increase in activity following aversive stimuli (Cohen et al., 2012; Tan et al., in press). Importantly, GABAergic neurotransmission in the VTA is drastically altered by exposure to drugs of abuse (Bonci and Williams, 1997; Johnson and North, 1992a; Madhavan et al., 2010; Nugent et al., 2007), which may result in aberrant activity in DA neurons, and which could promote maladaptive behaviors. While neurotransmission between VTA DA and GABA neurons may modulate reward processing, it is unknown if the activity of VTA GABA neurons influences motivated behavior, as manipulation of genetically distinct populations of VTA neurons has been difficult due to cellular heterogeneity. In the present study, we used optogenetic strategies to selectively stimulate VTA GABA neurons as well as their projection fibers to the NAc to determine whether the activity of these neurons could alter reward-seeking behavior as well as the excitability of neighboring DA neurons.

## Results

### Optogenetic stimulation of VTA GABA neurons

To selectively stimulate VTA GABA neurons, we injected a Cre-inducible adeno-associated viral construct, coding for ChR2-eYFP or eGFP (Tsai et al., 2009) unilaterally into the VTA of adult *VGat*-ires-Cre mice (Vong et al., 2011). 21 – 28 d later, robust expression of ChR2-eYFP was localized to the VTA (Figure 1A). Immunohistochemical staining to label tyrosine hydroxylase (TH), a marker for DA neurons, as well as the vesicular GABA transporter (VGAT), revealed that ChR2-eYFP-expressing fibers throughout the VTA were co-labeled for VGAT, suggesting that fibers from targeted neurons could release GABA (Figure 1B). Quantification of fluorescently labeled (but not all) VTA neurons revealed that 70.4 ± 1.3% were TH+, 29.6 ± 1.3% were eGFP+, and that 0.24 ± 0.20% co-labeled for both (n = 6 sections from n = 3 mice; Figures 1C - F). To determine the extent to which ChR2-eYFP positive fibers from VTA GABA neurons innervate the VTA vs. the neighboring Substantia Nigra pars compacta (Sn), we quantified eYFP fluorescence localized in these two regions. Robust ChR2-eYFP expression was observed in the VTA (Figures 1A,B,G), while significantly less fluorescent signal was detected in the Sn (Figures 1H,I), demonstrating that fibers from VTA GABA neurons densely innervate the VTA, but also sparsely innerve the Sn. To functionally demonstrate that VTA GABA neurons were optically excitable, we performed whole cell current clamp recordings from fluorescent-identified GABA neurons in VTA brain slices. Application of a 473 nm, 1 mW light pulse for 5 s, led to a sustained increase in the firing rate of these neurons (n = 4 neurons; Figures

1J,K). These data demonstrate that optical stimulation in these mice results in selective activation of VTA GABA neurons, which exhibit sustained firing at high frequencies (~60 Hz), consistent with previously reported evoked firing rates from VTA GABA neurons (Steffensen et al., 1998), and unidentified VTA neurons (Kiyatkin and Rebec, 1998).

### Timelocked activation of VTA GABA neurons during cue-evoked reward seeking

Since VTA neurons are thought to encode properties of rewards and predictive cues, we next determined the consequences of VTA GABA activation at key time points in a cue-reward conditioning task. ChR2-eYFP was selectively expressed in VTA GABAergic neurons and implantable optical fibers (Sparta et al., 2011) were secured unilaterally into brain tissue above the VTA (Supplementary Figure 1). Following recovery from surgery mice were trained in daily cue-reward conditioning sessions, which consisted of 40 trials (60 – 120 s inter-trial interval) where a 5 s tone/light stimulus predicted the delivery of 20 μl of a 10% sucrose solution. Following ~25 training sessions, mice displayed consistent anticipatory licking during cue presentation, as well as reward consummatory licking after the reward delivery (Figure 2A). On subsequent conditioning sessions, VTA GABA neurons were optically excited either during the 5 s cue presentation period, or during the first 5 s following reward delivery. Activation of VTA GABA neurons during the 5 s cue period did not alter either anticipatory or reward consummatory licking (Figures 2B,D,F) compared to behavioral sessions where laser pulses were delivered through the fiber optic cable, but light was not permitted to enter the brain. Interestingly, VTA GABA activation during the 5 s period following reward delivery significantly decreased reward consummatory licking, which then rebounded in the 5 s after termination of VTA GABA activation (Figures 2C,E,G). The ability of VTA GABA activation to disrupt reward consumption became even more pronounced if these neurons were optogenetically stimulated for 10 s (Supplementary Figure 2). Furthermore, 5 s GABA activation during the cue presentation did not alter the total number of licks over the entire behavioral session (Figure 2F), while activation following reward delivery significantly decreased the total number of licks (Figure 2G). In addition, when the 5 s optogenetic stimulation of VTA GABA neurons was applied every 30 s in an open field arena, we observed a reduction in movement velocity timelocked to optical activation, but no change in rotational locomotor behavior (Supplementary Figure 2). Taken together, these data demonstrate that activation of VTA GABA neurons following sucrose delivery selectively disrupts reward consumption.

### Activation of VTA GABA neurons or their forebrain projections during reward consumption

Next, we examined whether activation of VTA GABA neurons, or their projections to the NAc, could alter reward consumption in a task where mice were allowed free access to sucrose. ChR2-eYFP and optical fibers (Supplementary Figure 1) were targeted to VTA GABA neurons as described above. Mice were then trained in a free reward consumption task where they were allowed unlimited access to 10% sucrose for 20 min. Following stable daily sucrose intake, mice underwent sessions where they received a 5 s optical stimulation of VTA GABA neurons every 30 s. We then examined stimulation trials where the mice were actively engaged in licking in the 5 s preceding laser onset. VTA GABA stimulation significantly reduced free reward consumption during the time of the optical activation (Figure 3A,B). Light delivery to the VTA in wildtype littermates of *VGat*-ires-Cre mice, who received virus injections, but were not expressing ChR2-eYFP did not alter free reward consumption (Supplementary Figures 1, 3). In addition, burst analysis of licking timelocked to the optical stimulation revealed that VTA GABA activation decreased the duration of timelocked bout licking, but did not alter the inter-lick interval within a burst or the total number of lick bouts over the entire session. Lick bouts were defined as ≥ 4 licks occurring

within 1 s (Supplementary Figure 3). These data demonstrate that VTA GABA activation can disrupt free reward consumption by inducing early termination of a licking bout.

In addition to VTA GABA neurons signaling locally within the VTA, they also send long distance projections to forebrain targets such as the NAc (Van Bockstaele and Pickel, 1995), a brain region critical for consummatory behaviors (Hanlon et al., 2004; Kelley, 2004; Krause et al., 2010). We therefore determined whether activation of VTA GABA projections to the NAc could also disrupt reward consumption. ChR2-eYFP expressing fibers were observed in striatal targets following virus delivery to the VTA in *VGat*-ires-Cre mice (Figure 3C). We then quantified eYFP fluorescence in the NAc, dorsal medial striatum (DMS) and the dorsal lateral striatum (DLS) 6 weeks after virus injection into the VTA. Fluorescent signal, indicative of the density of GABAergic fibers originating from the VTA, was significantly higher in the NAc compared to either the DMS or DLS (Figure 3C). Importantly, whole-cell voltage clamp recordings from NAc neurons in close proximity to fluorescent fibers revealed that $GABA_A$ mediated inhibitory postsynaptic currents (IPSCs) were detected following optical stimulation of ChR2 (Figure 3D). This demonstrates that NAc synapses arising from VTA GABA neurons are capable of functionally inhibiting postsynaptic NAc neurons when they are optically stimulated. Interestingly, direct activation of VTA GABAergic projections to the NAc (via an optical fiber located in the NAc, Supplementary Figure 4) did not alter reward consumption timelocked to the optical stimulation (Figure 3E,F), despite using optical stimulation parameters calculated to activate ChR2 within 1 $mm^3$ from the tip of the optical fiber. This demonstrates that activation of VTA GABAergic projections in the NAc alone is not sufficient to suppress reward consumption. However, VTA-to-NAc GABA may still act in conjunction with intra-VTA GABA or GABA release in other project targets to suppress reward consumption.

## DA neuron excitability and activity during optical activation of VTA GABA neurons

Since direct activation of VTA GABA neurons, but not their projections to the NAc reduced reward consumption, we next explored the mechanisms by which VTA GABA stimulation could alter the activity and excitability of VTA DA neurons. We performed *ex vivo* whole-cell voltage and current clamp recordings from VTA DA neurons while optically stimulating VTA GABA neurons. Optical stimulation of VTA GABA neurons led to detectable IPSCs in VTA DA neurons that were abolished by bath application of the $GABA_A$ receptor antagonist, Gabazine (Figure 4A). To examine the effects of optical activation of VTA GABA neurons on the excitability and activity of VTA DA neurons, the membrane potentials of DA neurons were initially set to −60 mV in current clamp. 5 s current injection ramps were then applied through the patch pipette to evoke firing in the presence and absence of 5 s light pulse to activate VTA GABA neurons. Activation of VTA GABA neurons reduced excitability of VTA DA neurons as indicated by a significant increase in the rheobase of the recorded neurons compared to recordings when no stimulation occurred (Figure 4B,C). In addition, VTA GABA stimulation reduced the activity of VTA DA neurons as indicated by an increase in the inter-spike interval and a reduction in total number of spikes evoked by the current injection (Figure 4B,D,E). Furthermore, to determine if activation of VTA GABA neurons could functionally suppress activity-dependent release of NAc DA *in vivo*, we performed fast-scan cyclic voltammetry experiments in anesthetized mice. Electrical activation of VTA DA neurons resulted in a stimulation frequency dependent increase in detected NAc DA release, which was significantly attenuated by coincidental 5s VTA GABA activation that started 2.5 s before the electrical stimulation of the VTA (Figure 5). Taken together, these data demonstrate that activation of VTA GABA neurons reduces the excitability and evoked activity of neighboring VTA DA neurons *in vitro* and *in vivo*.

## Discussion

The activity of VTA neurons and subsequent release of DA, glutamate (Stuber et al., 2010; Tecuapetla et al., 2010; Yamaguchi et al., 2011), and GABA in forebrain targets such as the NAc are important processes that promote crucial aspects of motivated behavior. Thus, the regulation of DA neuronal activity, by both intrinsic and extrinsic mechanisms, is required for optimal behavioral performance. Further, the mechanisms that regulate DA neuronal activity in adaptive contexts may underlie maladaptive actions and responses that are seen in addiction and neuropsychiatric illnesses. In this study, we show that brief activation of VTA GABA neurons selectively disrupts reward consumption, when these neurons are stimulated following reward delivery, but not when they are activated during reward-predictive cue presentation. In well-trained animals, DA neurons display a transient high frequency burst of activity in response to the onset of reward predictive cues, followed by low frequency firing following reward delivery (Day et al., 2007; Mirenowicz and Schultz, 1996; Pan et al., 2005; Stuber et al., 2008; Tobler et al., 2005; Waelti et al., 2001). The endogenous burst activity of DA neurons is at least partially regulated by NMDA activation, likely induced by excitatory VTA afferents (Chergui et al., 1993; Deister et al., 2009; Johnson et al., 1992; Overton and Clark, 1992; Zweifel et al., 2009). Pharmacological blockade of $GABA_A$ receptors can also induce burst firing of DA neurons (Paladini et al., 1999; Paladini and Tepper, 1999), although this is likely because spontaneous excitatory activity onto DA neurons becomes dominant (i.e. disrupted excitatory/inhibitory balance). Importantly, single non-burst action potentials recorded from DA neurons are more efficiently blocked by GABA activation compared to spikes that occur in bursts (Lobb et al., 2010). Thus, it is possible that VTA GABA neuronal activity and other neurotransmitters in the VTA may not efficiently suppress the activity of VTA DA neurons at times when they are receiving excitatory afferent activation that drives bursting. Supporting this, in the current study we found that VTA GABA activation is less efficacious at suppressing NAc DA release *in vivo* when VTA DA neurons are excited at higher stimulation frequencies (Figure 5). Importantly, it was recently demonstrated that VTA GABA neurons show enhanced activity during a cue that predicts a reward (Cohen et al., 2012). This might explain why VTA GABA activation during the cue period in the current study did not alter licking behavior, as these neurons might already be endogenously activated and thus are less susceptible to further depolarization at this time. Overall, these reasons could explain why in the current study, optogenetic stimulation of VTA GABA neurons did not affect behavioral responding to reward predictive cues, but could disrupt behavioral responding at a time when DA and GABA neurons would be predicted to be firing at basal levels.

According to the reward-prediction error hypothesis of DA function (Schultz, 1998), efficient inhibition of VTA DA neuronal activity following reward delivery would not only disrupt reward consumption, but would also alter anticipatory responding to predictive cues on subsequent trials. In the present study, we did not observe a reduction in anticipatory licking when VTA GABA neurons were activated during the 5 s following reward delivery. However, with an even stronger stimulation, lasting 10 s following reward delivery, a trend for a decrease in cue-evoked licking was observed (Supplementary Figure 2). It is likely that anticipatory responses were not affected here because mice would immediately return and consume the awaiting reward upon the termination of the optical stimulation, which is distinct from reward omission that was used in previous electrophysiological studies. Although we show in this study that VTA GABA activation decreases NAc DA transients, it is important to note that we also observed fibers originating from VTA GABA neurons in the Sn as well as striatal regions. While, innervation from VTA GABA neurons to the Sn is sparse compared to innervation in the VTA (Figure 1), functional activation of these fibers in the Sn may still induce behaviorally relevant effects, such as the decrease in movement velocity that we observed timelocked to the optical stimulation (Supplementary Figure 2). It

should thus be taken into account that the effects on consummatory behavior might also be movement related, however, we would expect to observe similar reductions in anticipatory licking, which were not observed. It is important to note that DAergic projections from the Sn to the DLS are thought to also contribute to reward consummatory behavior, as depleting nigrostriatal DA decreases consummatory behavior (Cousins et al., 1993; Salamone et al., 1993; Salamone et al., 1990; Ungerstedt, 1971). Furthermore, restoring dorsal striatal DA signaling promotes feeding in aphagic DA deficient mice (Szczypka et al., 2001). On the other hand, selectively decreasing NAc DA signaling through specific neuronal depletion (Cousins et al., 1993; Salamone et al., 2001) or by local action of D1 or D2 antagonists (Ikemoto and Panksepp, 1996; Nowend et al., 2001) decreases motivation for earning food rewards, but not actual consumption. Taken together, these data suggest that movement, motivation, and reward consumption are interdependent processes, which all require DA signaling in striatal subregions.

Interestingly, the cessation of reward consumption occurred only when VTA GABA neurons were directly activated. While the NAc clearly plays an important role in mediating motivated behavioral responding (Kelley, 2004; Stuber et al., 2011), it seems that reward consumption *per se* cannot be altered by the activation of VTA GABA inputs to the NAc alone. Here, we chose to investigate the VTA GABAergic projection to the NAc because the NAc contained the largest amount of VTA GABA fibers in the striatum, and has been widely implicated in appetitive behavior (Hanlon et al., 2004; Kelley, 2004; Krause et al., 2010). While our results suggest that activation of VTA GABAergic inputs to the NAc alone does not reduce reward consumption, this does not rule out the possibility that other VTA GABAergic projections, such as those to the medial prefrontal cortex, may play a role in modulating reward seeking. Furthermore, although we show that activation of VTA GABA neurons directly alters the activity of neighboring VTA DA neurons, as well as the release of DA in the NAc, we cannot rule out that activating VTA GABA neurons results in additional changes in DA signaling in other forebrain target regions, other than the NAc, that could also play a role in the cessation of reward consumption.

While VTA GABA activation disrupts reward consumption, activation of these neurons can also cause a conditioned place aversion (Tan et al., submitted). It is possible that VTA GABA activation disrupts reward consumption and promotes aversive behaviors by distinct VTA GABA circuits or that activation of these neurons has other uncharacterized effects. Alternatively, enhanced activity of VTA GABA neurons may induce an acute anhedonia-like phenotype that would result in both aversive behaviors as well as a reduction in motivated behaviors, which could both occur by VTA GABA neurons directly inhibiting DA neuronal function. This idea is consistent with data that have implicated VTA DA neurons in aversive and anhedonic signaling (Bromberg-Martin et al., 2010; Nestler and Carlezon, 2006; Ungless et al., 2010). Thus, it is likely that multiple circuit-wide signaling modalities, including the interplay between VTA DA and GABA activity, are required for the initiation of aversion-related and the termination of reward-related behaviors.

## Experimental Procedures

### Animals and stereotactic surgery

Adult (25–40g) male VGat-ires-Cre mice backcrossed to C57BL/6J and wildtype littermates were group-housed until surgery (n = 26 for behavioral experiments; n = 7 for electrophysiological experiments; n = 6 for immunohistochemistry and microscopy experiments for colocalization of TH and ChR2-eYFP). For quantification of ChR2-eYFP fibers in the VTA and Sn as well as fibers in the NAc, DMS, and DLS, tissue from the mice used in the behavioral experiments were used. All mice were maintained on a 12:12 reverse light cycle (lights off at 08:00). Mice were anesthetized with 100 mg/kg ketamine 10 mg/kg

xylazine and placed in a stereotaxic frame (Kopf Instruments). Microinjection needles were then inserted unilaterally directly above the VTA (coordinates from Bregma: −3.1 AP, ±0.3 ML, −5.1DV). Microinjections were performed using custom-made injection needles (26 gauge) connected to a 2 μl Hamilton syringe. Each VTA was injected with 0.3 – 0.5 μl of purified AAV ($7.5 \times 10^{11}$ to $3 \times 10^{12}$ units/mL as described previously, (Stuber et al., 2011)) coding for Cre-inducible ChR2-eYFP, or eGFP under control of the EF1α promoter, over 3–5 minutes followed by an additional 10 minutes to allow diffusion of viral particles away from the injection site. For *in vivo* optical stimulation experiments mice were first injected unilaterally in the VTA with virus and then implanted with a chronic optical fiber directly above either the ipsilateral VTA or NAc (+1.0 AP, ±1.0 ML, −4.0 DV), as described previously (Sparta et al., 2011; Stuber et al., 2011). Implanted optical fibers were secured in place using skull screws and acrylic cement. Mice were then returned to their home cage. Body weight and signs of illness were monitored until recovery from surgery. Mice for electrophysiological and immunohistochemistry experiments were used > 21 d after surgery. For behavioral experiments, mice began behavioral training 14 – 21 d after surgery, but did not undergo optical stimulation sessions until > 31 d after surgery. All procedures were conducted in accordance with the Guide for the Care and Use of Laboratory Animals, as adopted by NIH, and with approval of the UNC Institutional Animal Care and Use Committee.

## Preparation of optical fibers

For a detailed account of the construction of implantable optical fibers and optical patch cables, see (Sparta et al., 2011). Briefly, for chronic fibers 200 μm core, 0.37 NA standard multimode hard cladding fiber (Thor Labs) was stripped of the cladding, threaded through a 230 μm multimode zirconia ferrule, polished and cut to a length of 6 mm. They were then tested for light output and sterilized using 70% ethanol before implantation into the brain. Optical patch cables connecting the fiber optic rotary joint to the chronic fiber consisted of a 60 μm core multimode fiber (0.22 NA), threaded through furcation tubing, connected to a 127 μm ID bore ceramic zirconia ferrule and a multimode FC multimode ferrule assembly (Precision Fiber products). Optical patch cables connecting the fiber optic rotary interfaced to the laser housing consisted of FC multimode ferrule assemblies on both ends. Light transmission was measured for all implantable optical fibers before implantation and after the animal was sacrificed. Only optical fibers with > 80% light transmission prior to implantation were used.

## Cue-reward conditioning task

2 – 3 week after AAV-Ef1a-DIO-ChR2-eYFP virus injection and fiber implantation into the VTA, male VGAT-ires-CRE mice were food restricted to 85 – 90% of their free-feeding bodyweight. Mice were food restricted for three days, while also tethered to custom-made optical patch cables for 1hr/day before they were trained for habituation purposes. Mice were then trained in sound attenuated mouse chambers (Med Associates) equipped with a white noise and tone generator, cue lights, and a receptacle for sucrose delivery that could detect head entries and individual licks. Mice were trained for one session per day that lasted ~ 60 min. Each session consisted of 40 trials where a randomized 60–120 s inter-trial interval followed by a 5 s tone/light cue presentation that terminated with delivery of 20 μL of a 10% sucrose solution. During each training session the chronic optical fiber was connected to a patch cable, interfacing with a FC/PC fiber optic rotary joint (Doric Lenses) which then interfaced with a 473 nm solid state laser outside the chamber. Mice were trained for 20 – 25 d until stable responding was observed to both cue and reward presentation. After training, mice underwent behavioral sessions where they received a 5 s laser stimulation (12 mW into the brain) starting either at the onset of the cue or the reward delivery in a counterbalanced fashion. Laser stimulation sessions were always flanked by

non-stimulation sessions on the previous and following days, where the laser light was blocked from reaching the brain by a piece of material that prevented light transmission inside the connecter sleeve connecting the optical patch cable to the chronic fiber. Cue onset, reward delivery, lick, and port entry timestamps were recorded with MED-PC (Med Associates) software and analyzed using NeuroExplorer (Nex Technologies) and Excel (Microsoft).

### Free reward consumption task

Following injection of AAV-Ef1a-DIO-ChR2-eYFP virus and fiber placement in VTA or NAc, mice were allowed to recover for 14 d. Mice were then food restricted to 85 – 90% of their original bodyweight over the course of the next 3–5 d. Next, mice were trained in chambers similar to those used in the cue-reward task, except that they were now equipped with bottle lickometers for quantification of free sucrose drinking. The free reward consumption task consisted of unlimited access to 10% sucrose for each 20 min session. Lick timestamps were recorded and used for analysis. Mice were trained until the number of licks made in each session was stable (<15% change) for 3 consecutive sessions, which for all mice occurred after 10 – 17 training sessions. In subsequent optical stimulation sessions, mice received a 5 s constant laser stimulation (with identical parameters to stimulations used in the cue-reward conditioning task) every 30 s during the task. Laser stimulation sessions were always flanked by sessions where laser delivery to the brain was blocked as described above. For analysis, only stimulations in which the mice were actively licking within the 5 s preceding optical stimulation were used, to ensure that the mice were actively engaged in reward consumption. For licking bout analysis, bouts were defined as bursts of licks where a minimum of 4 licks were recorded in 1 s.

### Open field velocity and rotation measurements

~1 week following completion of the cue-reward conditioning experiment, a subset of mice were tethered to an optical cable and placed in a 10 inch by 10 inch plastic arena that had 10 inch walls. The arena contained regular bedding and was placed in a dark enclosed chamber. During 20 minutes their activity was recorded by an infrared camera, where they either received 5s of optical stimulation every 30s or in the same interval they received control stimulations were the laser light was blocked from reaching the brain. All 6 mice received both treatments on consecutive days, in a randomized fashion. Recorded video tracks were then analyzed using Ethovision (Noldus Information Technology) and Matlab (Mathworks).

### Slice preparation for patch-clamp electrophysiology

Mice were anesthetized with pentobarbital and perfused transcardially with modified aCSF containing (in mM): 225 sucrose, 119 NaCl, 2.5 KCl, 1.0 $NaH_2PO_4$, 4.9 $MgCl_2$, 0.1 $CaCl_2$, 26.2 $NaHCO_3$, 1.25 glucose. The brain was removed rapidly from the skull and placed in the same solution used for perfusion at ~0°C. Horizontal sections of the VTA (200 μm) were then cut on a vibratome (VT-1200, Leica Microsysytems). Slices were then placed in a holding chamber and allowed to recover for at least 30 min before being placed in the recording chamber and superfused with bicarbonate-buffered solution saturated with 95% O2 and 5% $CO_2$ and containing (in mM): 119 NaCl, 2.5 KCl, 1.0 $NaH_2PO_4$, 1.3 $MgCl_2$, 2.5 $CaCl_2$, 26.2 $NaHCO_3$, and 11 glucose (at 32 – 34°C).

### Patch-clamp electrophysiology

Cells were visualized using infrared differential interference contrast and fluorescence microscopy. Whole-cell voltage-clamp or current clamp recordings of VTA DA or GABA neurons or NAc neurons were made using an Axopatch 700B amplifier. Patch electrodes (3.0 – 5.0 MΩ) were backfilled with internal solution for current clamp recordings

containing (in mM): 130 K-Gluconate, 10 KCl, 10 HEPES, 10 EGTA, 2 $MgCl_2$, 2 ATP, 0.2 GTP. For voltage clamp recordings the internal solution contained (in mM): 130 CsCl, 1 EGTA, 10 HEPES, 2 ATP, 0.2 GTP (pH 7.35, 270–285 mOsm for both internal solutions). Series resistance (15 – 25 MΩ) and/or input resistance were monitored online with a 4 mV hyperpolarizing step given between stimulation sweeps. All data were filtered at 2 kHz, digitized at 5 – 10 kHz, and collected using pClamp10 software (Molecular Devices). For current clamp experiments in fluorescently identified VTA GABA neurons, membrane potentials were initially maintained at −70 mV, and 5 s 473 nm, 1 mW light pulse delivered through a 40x objective via a high powered LED (Thorlabs) to evoked neuronal firing. VTA DA neurons were identified by their lack of fluorescence, and the presence of an $I_h$ current as described previously (Stuber et al., 2008). A subset of neurons were also filled with Alexa 594 (20 μg/mL; Invitrogen) and immunostained for TH to ensure they were DAergic. For voltage clamp recordings of optically evoked IPSCs in both DA neurons as well as NAc neurons, the cells were held at −70 mV, and a 1 – 5 ms, 473 nm, 1 mW light pulse was delivered to the tissue every 20 s. Following 5 – 10 min of baseline responding 10 μM of the $GABA_A$ receptor antagonist, SR-95531 (Gabazine), was bath applied for an additional 10 min. IPSC amplitudes were calculated by measuring the peak current from the average IPSC response from 6 sweeps during the baseline and 6 sweeps following Gabazine application. Cells that showed a > 20% change in the holding current or access resistance, were excluded from analysis. For whole cell current clamp recordings from DA neurons, membrane potentials were initially set to −60 mV at the start of the experiment and in between sweeps. Somatic current injection ramps (+100 pA over 5 s) were applied every 30 s. Recorded cells were exposed to 5 sweeps with no light stimulation, and 5 sweeps with 5 s light stimulation applied for the duration of the current injection ramp. Sets of sweeps with light and no light stimulation were counterbalanced across cells. Rheobase (the amount of current required for the first observed action potential), inter-spike interval, and the number of evoked spikes were computed by averaging these measurements across the 5 sweeps with or without light stimulation.

### In vivo fast-scan cyclic voltammetry

Fast-scan cyclic voltammetry (FSCV) experiments were conducted using method described in previous studies (Tsai et al., 2009). Briefly, mice were anesthetized with ketamine/xylazine (as described above) and placed in a stereotaxic frame. A craniotomy was done above the NAc (AP, +1.0 mm; ML, 1.0 mm) and the VTA (AP, −3.1 mm; ML, 0.3 mm). An Ag/AgCl reference electrode was implanted in the contralateral forebrain. An optical fiber, used for stimulating ChR2-expressing VTA GABA neurons, was coupled (0.5 mm above and 1 mm posterior) to a bipolar stimulating electrode. The stimulating optrode was then placed in a way that the electrical stimulating electrode was ~1mm anterior to the VTA (DV, −4.6 and −5.1 mm for optical fiber and stimulating electrode, respectively). A carbon fiber electrode (~100 μm in length) for voltammetric recordings was then lowered into the NAc (DV, −4.0 mm) in 0.25 mm intervals. Voltammetric measurements were made every 100 ms by application of a triangle waveform (−0.4 V to +1.3 V to −0.4 V vs. Ag/AgCl, at 400 V/s) to the carbon fiber electrode. DA release was evoked by electrical activation of the VTA DA cell bodies using 20 pulse-stimulation (4 ms single pulse duration) with frequencies between 5 and 60 Hz. The stimulating current was maintained at 300 μA. An optical stimulation of ChR2-expressing VTA GABA neurons was applied for 5 s starting 2.5 s before the onset of electrical stimulus. Recorded voltammetric signals showed an oxidation peak at +0.65 V and a reduction peak at −0.2 V (vs. Ag/AgCl reference), as well as characteristic cyclic voltammograms, ensuring that the released chemical was DA. Carbon fiber electrodes were calibrated *in vitro* with known concentrations of DA (0.2, 0.5 and 1.0 μM). Calibrations were done in duplicate and the average value for the current at the peak oxidation potential

was used to normalize *in vivo* signals to DA concentration. All voltammetry data was analyzed using TarHeel CV software.

### Histology, immunohistochemistry, and microscopy

Mice were deeply anesthetized with pentobarbital and transcardially perfused with phosphate-buffered saline (PBS) followed by 4% paraformaldehyde (Sigma) in PBS. Brains were then harvested and submerged in 4% paraformaldehyde for 48 hrs, then transferred to 30% sucrose in $ddH_20$ for 72hrs. 40 μm sections were obtained on a cryostat (Leica) and processed immunohistochemically for visualization of neuronal cell bodies, VGAT, and/or TH expression. Neuronal cell bodies were stained with Neurotrace (Invitrogen; 640nm excitation/660nm emission) using previously adopted methods (Stuber et al., 2011). Briefly, sections were washed in 0.1% Triton (Sigma) in PBS for 10 min, followed by two 5 min washes of PBS before staining in 2% Neurotrace for 1hr at room temperature. Sections were then washed in 0.1% Triton for another 10 min before the final two washes of PBS for 5 min each. For visualization of VGAT (Millipore; made in Rabbit) and TH (Pel Freeze; made in Sheep) expression, sections were washed in 0.5% Triton in PBS, followed by one PBS wash, and then blocked in 10% normal donkey serum in 0.1% Triton for 1hr. Primary antibodies were added (VGAT, 1:2000; TH 1:500) directly to blocking solution and incubated at 4°C for 48 hrs,, then was hed 4 times in PBS. Sections were then transferred to secondary antibody (Jackson Immunoresearch; donkey anti-rabbit 405, donkey anti-sheep 649) in PBS according to manufacturer recommended dilutions and incubated at room temperature for 2 hr prior to washing 4 times in PBS. Sections were mounted on 1 mm Superfrost slides (Fisher) and mounted with Vectashield (Vector Labs) mounting medium. Z-stack, tiles, and single images were acquired on a Zeiss LSM Z10 confocal microscope using a 20x, 40x, or 63x objectives and analyzed using ZEN 2009 and Image J software. For cell counting, images were marked/counted using digital image editing software. For quantification of ChR2-eYFP fluorescence intensity, images were acquired using identical pinhole, gain, and laser settings for the NAc, DMS, and DLS sections, and for the VTA and Sn sections. No additional post-processing was performed on any of the collected images. ChR2-eYFP fluorescence intensity was then quantified using a scale from 0 – 255 in Image J to determine the mean intensity across the entire image. For determination of optical fiber placements, tissue was imaged at 10x and 20x on an upright conventional fluorescent microscope. Optical stimulation sites were recorded as the location in tissue 0.5 mm more ventral than where visible optical fiber tracks terminated.

### Data analysis and statistics

Behavioral data was analyzed using Neuroexplorer, Microsoft Excel, and Prism. Electrophysiological data was analyzed in ClampFit and Prism. Voltammetry data was analyzed with TarHeel CV. Imagining data was analyzed with ZEN 2009 and Image J. Between and within subjects t-tests, and ANOVAs followed by Bonferroni post-hoc tests were used when applicable with an $\alpha = 0.05$.

## Supplementary Material

Refer to Web version on PubMed Central for supplementary material.

## Acknowledgments

We thank Drs. Bradford Lowell and Linh Vong for providing the *VGat*-ires-Cre mice and Dr. Karl Deisseroth for AAV-DIO-ChR2-eYFP, and AAV-DIO-GFP constructs. We also thank Randall Ung and Dr. Vladimir Gukassyan and the UNC Neuroscience Center Microscopy Core Facility for assistance. This study was supported by funds from NARSAD, The Whitehall Foundation, The Foundation of Hope, NIDA (DA029325 and DA032750), and startup funds provided by the Department of Psychiatry at UNC Chapel Hill (G.D.S.), and DA021634 (E.A.B.).

R.v.Z. was supported by the Hendrik Muller Fonds, Fundatie van de Vrijvrouwe van Renswoude, David de Wied Stichting, and Vreedefonds.

## References

Adamantidis AR, Tsai HC, Boutrel B, Zhang F, Stuber GD, Budygin EA, Tourino C, Bonci A, Deisseroth K, de Lecea L. Optogenetic interrogation of dopaminergic modulation of the multiple phases of reward-seeking behavior. J Neurosci. 2011; 31:10829–10835. [PubMed: 21795535]

Bonci A, Williams JT. Increased probability of GABA release during withdrawal from morphine. J Neurosci. 1997; 17:796–803. [PubMed: 8987801]

Brischoux F, Chakraborty S, Brierley DI, Ungless MA. Phasic excitation of dopamine neurons in ventral VTA by noxious stimuli. Proc Natl Acad Sci U S A. 2009; 106:4894–4899. [PubMed: 19261850]

Bromberg-Martin ES, Hikosaka O. Midbrain dopamine neurons signal preference for advance information about upcoming rewards. Neuron. 2009; 63:119–126. [PubMed: 19607797]

Bromberg-Martin ES, Matsumoto M, Hikosaka O. Dopamine in motivational control: rewarding, aversive, and alerting. Neuron. 2010; 68:815–834. [PubMed: 21144997]

Chergui K, Charlety PJ, Akaoka H, Saunier CF, Brunet JL, Buda M, Svensson TH, Chouvet G. Tonic activation of NMDA receptors causes spontaneous burst discharge of rat midbrain dopamine neurons in vivo. Eur J Neurosci. 1993; 5:137–144. [PubMed: 8261095]

Cohen JY, Haesler S, Vong L, Lowell BB, Uchida N. Neuro-type-specific signalts for reward and punishment in the ventral tegmental area. Nature. 201210.1038/nature10754

Cousins MS, Sokolowski JD, Salamone JD. Different effects of nucleus accumbens and ventrolateral striatal dopamine depletions on instrumental response selection in the rat. Pharmacol Biochem Behav. 1993; 46:943–951. [PubMed: 8309975]

Day JJ, Roitman MF, Wightman RM, Carelli RM. Associative learning mediates dynamic shifts in dopamine signaling in the nucleus accumbens. Nature neuroscience. 2007; 10:1020–1028.

Deister CA, Teagarden MA, Wilson CJ, Paladini CA. An intrinsic neuronal oscillator underlies dopaminergic neuron bursting. J Neurosci. 2009; 29:15888–15897. [PubMed: 20016105]

Fields HL, Hjelmstad GO, Margolis EB, Nicola SM. Ventral tegmental area neurons in learned appetitive behavior and positive reinforcement. Annual review of neuroscience. 2007; 30:289–316.

Hanlon EC, Baldo BA, Sadeghian K, Kelley AE. Increases in food intake or food-seeking behavior induced by GABAergic, opioid, or dopaminergic stimulation of the nucleus accumbens: is it hunger? Psychopharmacology (Berl). 2004; 172:241–247. [PubMed: 14598017]

Ikemoto S, Panksepp J. Dissociations between appetitive and consummatory responses by pharmacological manipulations of reward-relevant brain regions. Behav Neurosci. 1996; 110:331–345. [PubMed: 8731060]

Jhou TC, Fields HL, Baxter MG, Saper CB, Holland PC. The rostromedial tegmental nucleus (RMTg), a GABAergic afferent to midbrain dopamine neurons, encodes aversive stimuli and inhibits motor responses. Neuron. 2009; 61:786–800. [PubMed: 19285474]

Johnson SW, North RA. Opioids excite dopamine neurons by hyperpolarization of local interneurons. J Neurosci. 1992a; 12:483–488. [PubMed: 1346804]

Johnson SW, North RA. Two types of neurone in the rat ventral tegmental area and their synaptic inputs. The Journal of physiology. 1992b; 450:455–468. [PubMed: 1331427]

Johnson SW, Seutin V, North RA. Burst firing in dopamine neurons induced by N-methyl-D-aspartate: role of electrogenic sodium pump. Science (New York, NY. 1992; 258:665–667.

Kelley AE. Ventral striatal control of appetitive motivation: role in ingestive behavior and reward-related learning. Neurosci Biobehav Rev. 2004; 27:765–776. [PubMed: 15019426]

Kiyatkin EA, Rebec GV. Heterogeneity of ventral tegmental area neurons: single-unit recording and iontophoresis in awake, unrestrained rats. Neuroscience. 1998; 85:1285–1309. [PubMed: 9681963]

Krause M, German PW, Taha SA, Fields HL. A pause in nucleus accumbens neuron firing is required to initiate and maintain feeding. J Neurosci. 2010; 30:4746–4756. [PubMed: 20357125]

Lobb CJ, Wilson CJ, Paladini CA. A dynamic role for GABA receptors on the firing pattern of midbrain dopaminergic neurons. J Neurophysiol. 2010; 104:403–413. [PubMed: 20445035]

Luscher C, Malenka RC. Drug-evoked synaptic plasticity in addiction: from molecular changes to circuit remodeling. Neuron. 2011; 69:650–663. [PubMed: 21338877]

Madhavan A, Bonci A, Whistler JL. Opioid-Induced GABA potentiation after chronic morphine attenuates the rewarding effects of opioids in the ventral tegmental area. J Neurosci. 2010; 30:14029–14035. [PubMed: 20962224]

Margolis EB, Lock H, Hjelmstad GO, Fields HL. The ventral tegmental area revisited: is there an electrophysiological marker for dopaminergic neurons? The Journal of physiology. 2006; 577:907–924. [PubMed: 16959856]

Matsumoto M, Hikosaka O. Two types of dopamine neuron distinctly convey positive and negative motivational signals. Nature. 2009; 459:837–841. [PubMed: 19448610]

Mileykovskiy B, Morales M. Duration of inhibition of ventral tegmental area dopamine neurons encodes a level of conditioned fear. J Neurosci. 2011; 31:7471–7476. [PubMed: 21593330]

Mirenowicz J, Schultz W. Preferential activation of midbrain dopamine neurons by appetitive rather than aversive stimuli. Nature. 1996; 379:449–451. [PubMed: 8559249]

Nair-Roberts RG, Chatelain-Badie SD, Benson E, White-Cooper H, Bolam JP, Ungless MA. Stereological estimates of dopaminergic, GABAergic and glutamatergic neurons in the ventral tegmental area, substantia nigra and retrorubral field in the rat. Neuroscience. 2008; 152:1024–1031. [PubMed: 18355970]

Nestler EJ, Carlezon WA Jr. The mesolimbic dopamine reward circuit in depression. Biol Psychiatry. 2006; 59:1151–1159. [PubMed: 16566899]

Nowend KL, Arizzi M, Carlson BB, Salamone JD. D1 or D2 antagonism in nucleus accumbens core or dorsomedial shell suppresses lever pressing for food but leads to compensatory increases in chow consumption. Pharmacol Biochem Behav. 2001; 69:373–382. [PubMed: 11509194]

Nugent FS, Penick EC, Kauer JA. Opioids block long-term potentiation of inhibitory synapses. Nature. 2007; 446:1086–1090. [PubMed: 17460674]

Overton P, Clark D. Iontophoretically administered drugs acting at the N-methyl-D-aspartate receptor modulate burst firing in A9 dopamine neurons in the rat. Synapse. 1992; 10:131–140. [PubMed: 1533955]

Paladini CA, Iribe Y, Tepper JM. GABAA receptor stimulation blocks NMDA-induced bursting of dopaminergic neurons in vitro by decreasing input resistance. Brain Res Brain Res Rev. 1999; 832:145–151.

Paladini CA, Tepper JM. GABA(A) and GABA(B) antagonists differentially affect the firing pattern of substantia nigra dopaminergic neurons in vivo. Synapse. 1999; 32:165–176. [PubMed: 10340627]

Pan WX, Schmidt R, Wickens JR, Hyland BI. Dopamine cells respond to predicted events during classical conditioning: evidence for eligibility traces in the reward-learning network. J Neurosci. 2005; 25:6235–6242. [PubMed: 15987953]

Phillips PE, Stuber GD, Heien ML, Wightman RM, Carelli RM. Subsecond dopamine release promotes cocaine seeking. Nature. 2003; 422:614–618. [PubMed: 12687000]

Roitman MF, Stuber GD, Phillips PE, Wightman RM, Carelli RM. Dopamine operates as a subsecond modulator of food seeking. J Neurosci. 2004; 24:1265–1271. [PubMed: 14960596]

Salamone JD, Mahan K, Rogers S. Ventrolateral striatal dopamine depletions impair feeding and food handling in rats. Pharmacol Biochem Behav. 1993; 44:605–610. [PubMed: 8451265]

Salamone JD, Wisniecki A, Carlson BB, Correa M. Nucleus accumbens dopamine depletions make animals highly sensitive to high fixed ratio requirements but do not impair primary food reinforcement. Neuroscience. 2001; 105:863–870. [PubMed: 11530224]

Salamone JD, Zigmond MJ, Stricker EM. Characterization of the impaired feeding behavior in rats given haloperidol or dopamine–depleting brain lesions. Neuroscience. 1990; 39:17–24. [PubMed: 2128534]

Schultz W. Predictive reward signal of dopamine neurons. J Neurophysiol. 1998; 80:1–27. [PubMed: 9658025]

Sparta DR, Stamatakis AM, Phillips JL, Hovelso N, van Zessen R, Stuber GD. Construction of implantable optical fibers for long-term optogenetic manipulation of neural circuits. Nature Protocols. 2011; 7:12–23.

Steffensen SC, Svingos AL, Pickel VM, Henriksen SJ. Electrophysiological characterization of GABAergic neurons in the ventral tegmental area. J Neurosci. 1998; 18:8003–8015. [PubMed: 9742167]

Stuber GD, Hnasko TS, Britt JP, Edwards RH, Bonci A. Dopaminergic terminals in the nucleus accumbens but not the dorsal striatum corelease glutamate. J Neurosci. 2010; 30:8229–8233. [PubMed: 20554874]

Stuber GD, Klanker M, de Ridder B, Bowers MS, Joosten RN, Feenstra MG, Bonci A. Reward-predictive cues enhance excitatory synaptic strength onto midbrain dopamine neurons. Science (New York, NY. 2008; 321:1690–1692.

Stuber GD, Sparta DR, Stamatakis AM, van Leeuwen WA, Hardjoprajitno JE, Cho S, Tye KM, Kempadoo KA, Zhang F, Deisseroth K, et al. Excitatory transmission from the amygdala to nucleus accumbens facilitates reward seeking. Nature. 2011; 475:377–380. [PubMed: 21716290]

Stuber GD, Wightman RM, Carelli RM. Extinction of cocaine self-administration reveals functionally and temporally distinct dopaminergic signals in the nucleus accumbens. Neuron. 2005; 46:661–669. [PubMed: 15944133]

Swanson LW. The projections of the ventral tegmental area and adjacent regions: a combined fluorescent retrograde tracer and immunofluorescence study in the rat. Brain Res Bull. 1982; 9:321–353. [PubMed: 6816390]

Szczypka MS, Kwok K, Brot MD, Marck BT, Matsumoto AM, Donahue BA, Palmiter RD. Dopamine production in the caudate putamen restores feeding in dopamine-deficient mice. Neuron. 2001; 30:819–828. [PubMed: 11430814]

Tan KR, Turiault M, Yvon C, Tye KM, Mirzabekov J, Doehner J, Labouebe G, Deisseroth K, Luscher C. GABA neurons of the VTA drive conditioned place aversion. Neuron. (accepted for publication).

Tecuapetla F, Patel JC, Xenias H, English D, Tadros I, Shah F, Berlin J, Deisseroth K, Rice ME, Tepper JM, et al. Glutamatergic signaling by mesolimbic dopamine neurons in the nucleus accumbens. J Neurosci. 2010; 30:7105–7110. [PubMed: 20484653]

Tobler PN, Fiorillo CD, Schultz W. Adaptive coding of reward value by dopamine neurons. Science (New York, NY. 2005; 307:1642–1645.

Tsai HC, Zhang F, Adamantidis A, Stuber GD, Bonci A, de Lecea L, Deisseroth K. Phasic firing in dopaminergic neurons is sufficient for behavioral conditioning. Science. 2009; 324:1080–1084. [PubMed: 19389999]

Ungerstedt U. Adipsia and aphagia after 6-hydroxydopamine induced degeneration of the nigrostriatal dopamine system. Acta Physiol Scand Suppl. 1971; 367:95–122. [PubMed: 4332694]

Ungless MA, Argilli E, Bonci A. Effects of stress and aversion on dopamine neurons: implications for addiction. Neuroscience and biobehavioral reviews. 2010; 35:151–156. [PubMed: 20438754]

Van Bockstaele EJ, Pickel VM. GABA-containing neurons in the ventral tegmental area project to the nucleus accumbens in rat brain. Brain Res. 1995; 682:215–221. [PubMed: 7552315]

Vong L, Ye C, Yang Z, Choi B, Chua S Jr, Lowell BB. Leptin action on GABAergic neurons prevents obesity and reduces inhibitory tone to POMC neurons. Neuron. 2011; 71:142–154. [PubMed: 21745644]

Waelti P, Dickinson A, Schultz W. Dopamine responses comply with basic assumptions of formal learning theory. Nature. 2001; 412:43–48. [PubMed: 11452299]

Wise RA. Dopamine, learning and motivation. Nature reviews. 2004; 5:483–494.

Yamaguchi T, Wang HL, Li X, Ng TH, Morales M. Mesocorticolimbic glutamatergic pathway. J Neurosci. 2011; 31:8476–8490. [PubMed: 21653852]

Zweifel LS, Fadok JP, Argilli E, Garelick MG, Jones GL, Dickerson TM, Allen JM, Mizumori SJ, Bonci A, Palmiter RD. Activation of dopamine neurons is critical for aversive conditioning and prevention of generalized anxiety. Nature neuroscience. 2011; 14:620–626.

Zweifel LS, Parker JG, Lobb CJ, Rainwater A, Wall VZ, Fadok JP, Darvas M, Kim MJ, Mizumori SJ, Paladini CA, et al. Disruption of NMDAR-dependent burst firing by dopamine neurons provides

selective assessment of phasic dopamine-dependent behavior. Proc Natl Acad Sci U S A. 2009; 106:7281–7288. [PubMed: 19342487]

## Highlights

- Activation of VTA GABA neurons following reward-delivery disrupts reward consumption.
- Activation of VTA GABA neurons during cue presentation does not alter anticipatory behavior.
- Activation of VTA GABA projections to the NAc does not alter reward consumption.
- The activity and excitability of VTA DA neurons are reduced by VTA GABA neuron stimulation *in vitro* and *in vivo*.

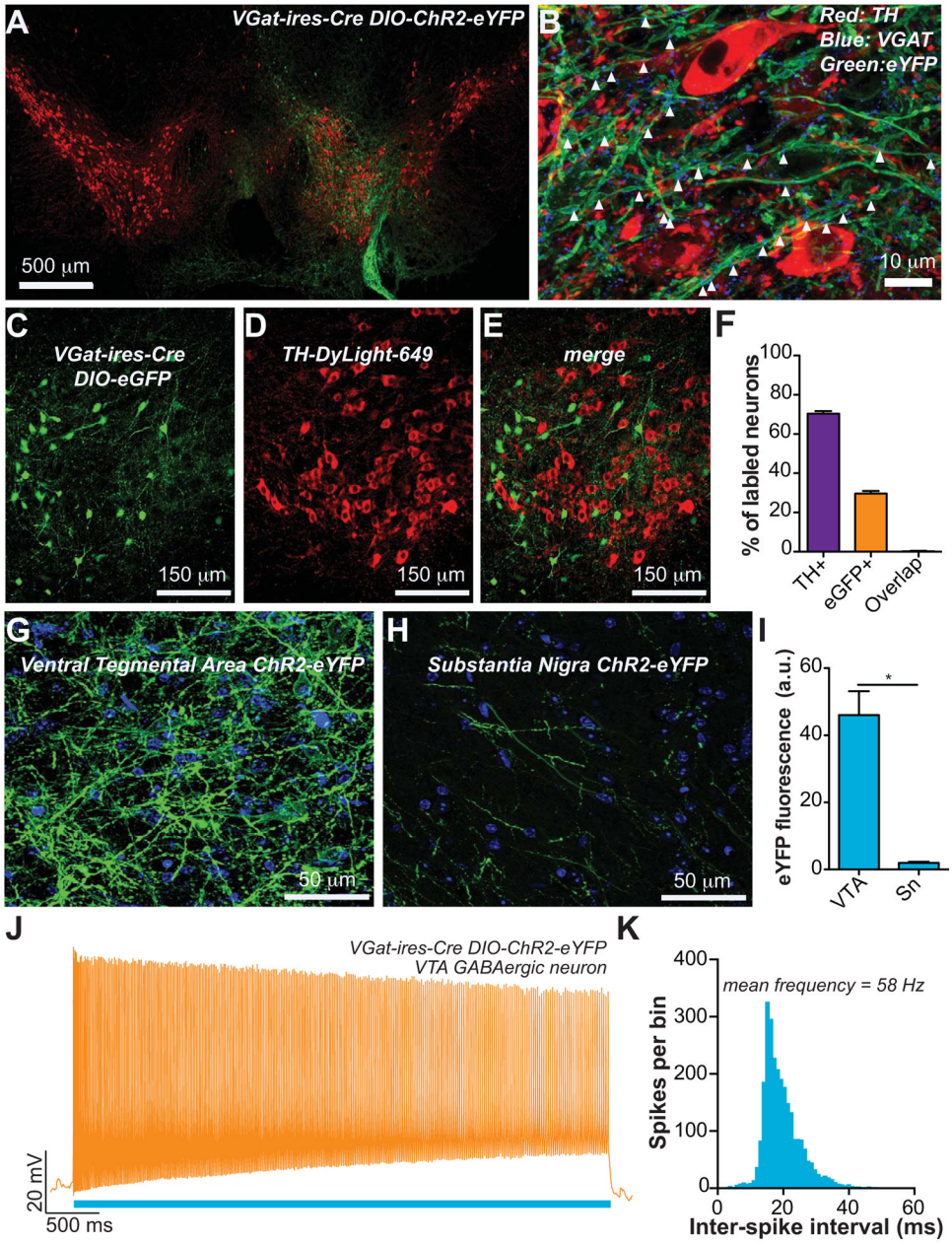


**Figure 1. Optogenetic stimulation of VTA GABA neurons**

(A) Expression of ChR2-eYFP following injection of the viral construct unilaterally into the VTA shown in green. Midbrain DA neurons, as indicated by tyrosine hydroxylase immunoreactivity, are shown in red. (B) Confocal compressed z-stack showing that ChR2-eYFP expressed in VTA fibers co-localizes with immunoreactivity for the vesicular GABA transporter. (C – F) Targeted eGFP expression in Cre expressing GABA neurons revealed minimal co-expression of TH in these neurons (n = 6 sections from n = 3 mice). (G,H) Confocal compressed z-stack showing ChR2-eYFP (green) in the VTA and Sn. DAPI counterstain shown in blue. (I) The average eYFP fluorescence intensity was significantly higher in the VTA compared to the Sn ($t(10) = 6.18$, $p = 0.0001$, n = 6 images per brain region from n = 6 mice). (J,K) Activation of ChR2 in VTA GABA neurons resulted in sustained high frequency activation during the 5 s stimulation (n = 4 neurons).

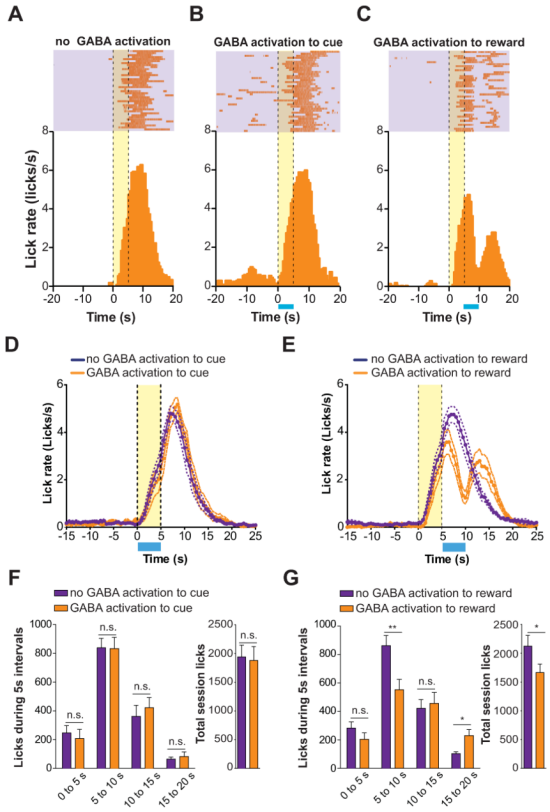


**Figure 2. Optical activation of VTA GABA neurons timelocked to reward delivery disrupts reward consumption**

(A) Example perievent histogram showing lick responses timelocked to reward-predictive cue (cue onset = 0 s; yellow bar) and reward delivery (occurring at t = 5 s) from a single mouse. Above raster plot indicates the licks made on each trial of the session (one trial per row). (B) Example perievent histogram showing data from a single mouse when VTA GABA neurons where activated (blue bar) during the reward predictive cue period (t = 0 – 5 s). (C) Example perievent histogram showing data from a single mouse when VTA GABA neurons where activated (blue bar) immediately following reward delivery (t = 5 – 10 s). (D) Average histogram data across all mice tested showing the change in the average lick rate when VTA GABA neurons where activated during cue presentation compared to sessions where mice did not receive optical stimulation. (E) Average histogram data across all mice tested showing the change in the average lick rate when VTA GABA neurons where activated immediately following reward delivery compared to sessions where mice did not receive optical stimulation. (F) Average data from (D) broken into 5 s time bins surrounding cue presentation (0 – 5 s) and reward consumption (5 – 10 s) periods (ANOVA for interaction: $F(3,56) = 0.24$, $p = 0.86$, n = 8 session per condition). Inset graph shows the average total session licks made during stimulation and non-stimulation sessions timelocked to cues ($t(7) = 0.35$, $p = 0.73$, n = 8 session per condition). (G) Average data from (E) broken into 5 s time bins surrounding cue presentation (0 – 5 s) and reward consumption (5 – 10 s) periods (ANOVA for interaction: $F(3,56) = 5.4$, $p = 0.002$, n = 8 session per condition). Inset graph shows the average total session licks made during stimulation and non-stimulation sessions timelocked to reward delivery ($t(7) = 2.9$, $p = 0.02$, n = 8 session per condition). Asterisks denote post-hoc statistical significance, * $p < 0.05$, ** $p < 0.01$.

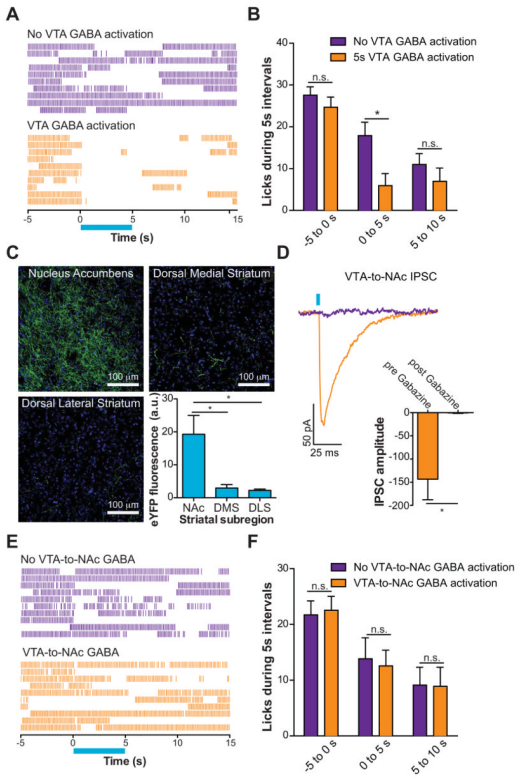


**Figure 3. Optical activation VTA GABA neurons but not their projections to the NAc disrupt free-reward consumption**

(A) Example raster plots showing free-reward licking immediately before, during, and after 5 s optical activation of VTA GABA neurons (blue bar). (B) Average data from all mice tested showing the number of licks made in the free reward consumption task surrounding the 5 s optical stimulation of VTA GABA neurons compared to blocked stimulation sessions (two-way ANOVA for a stimulation effect: $F(1,30) = 7.89$, $p = 0.009$, $n = 6$ mice). Asterisk denotes post-hoc statistical significance, $p < 0.05$. (C) Confocal image showing ChR2-eYFP expression in VTA GABAergic fibers innervating the NAc, DMS, and DLS (green). DAPI counterstain shown in blue. Average eYFP fluorescence intensity was significantly higher in the NAc compared to the DMS or DLS ($F(2,29) = 8.31$, $p = 0.002$, $n = 10$ images per brain region from $n = 5$ mice). Asterisk indicates $p < 0.05$. (D) Light evoked IPSCs via optical activation of VTA GABA fibers that innervate the NAc are blocked by bath application of 10 μM Gabazine ($t(3) = 3.3$, $p = 0.04$, $n = 4$ neurons). (E) Example raster plots showing free-reward licking immediately before, during, and after 5 s optical activation of VTA GABA fibers that project to the NAc. (F) Average data from all mice tested showing the number of licks made in the free reward consumption task surrounding the 5 s optical stimulation of VTA GABA projections to the NAc compared to blocked stimulation sessions (two-way ANOVA for a stimulation effect: $F(1,30) = 0.01$, $p = 0.93$, $n = 6$ mice).

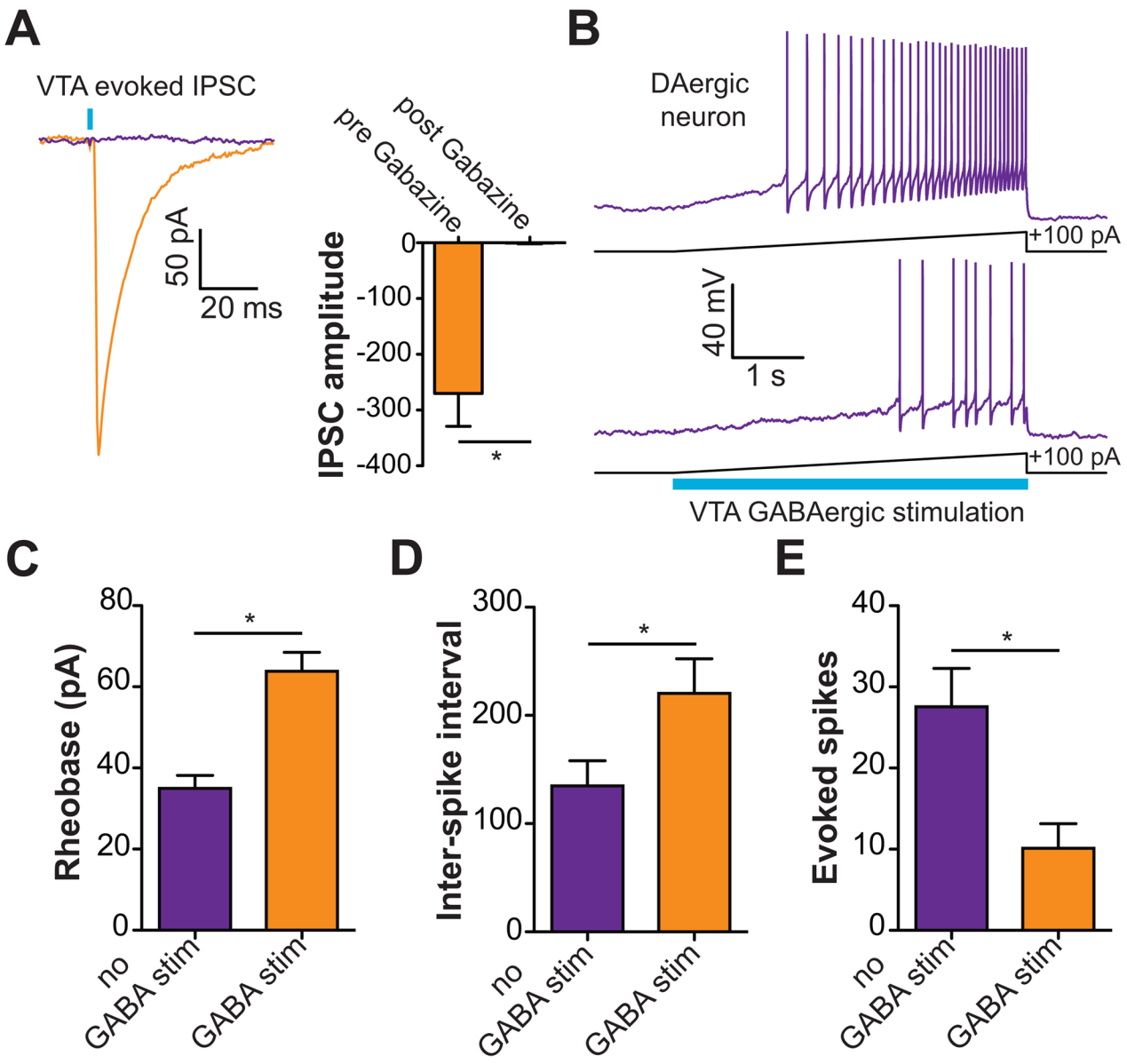


**Figure 4. Activation of VTA GABA neurons reduces the excitability of VTA DA neurons and the release of DA in the NAc**

(A) Light evoked IPSCs recorded from VTA DA neurons are blocked by bath application of 10 μM Gabazine ($t(4) = 4.5$, $p = 0.01$, $n = 5$ neurons). Asterisk indicates $p < 0.05$. (B) Current clamp recordings in DA neurons in response to +100 pA current injection ramps paired with a 5 s optical stimulation of VTA GABA neurons. The top trace shows the evoked firing in a neuron induced by the current injection; bottom trace shows the response in the same neuron when neighboring VTA GABA neurons are coincidentally activated. (C) VTA GABA activation decreases the excitability of VTA DA neurons as indicated by an increase in rheobase ($t(5) = 5.2$, $p = 0.004$, $n = 6$ neurons). Asterisk indicates $p < 0.05$. (D,E) VTA GABA activation decreases the activity of DA neurons as indicated by an increase in the inter-spike interval ($t(5) = 4.4$, $p = 0.007$, $n = 6$ neurons) and a decrease in the total number of evoked spikes ($t(5) = 6.7$, $p = 0.001$, $n = 6$ neurons). Asterisk indicates $p < 0.05$.

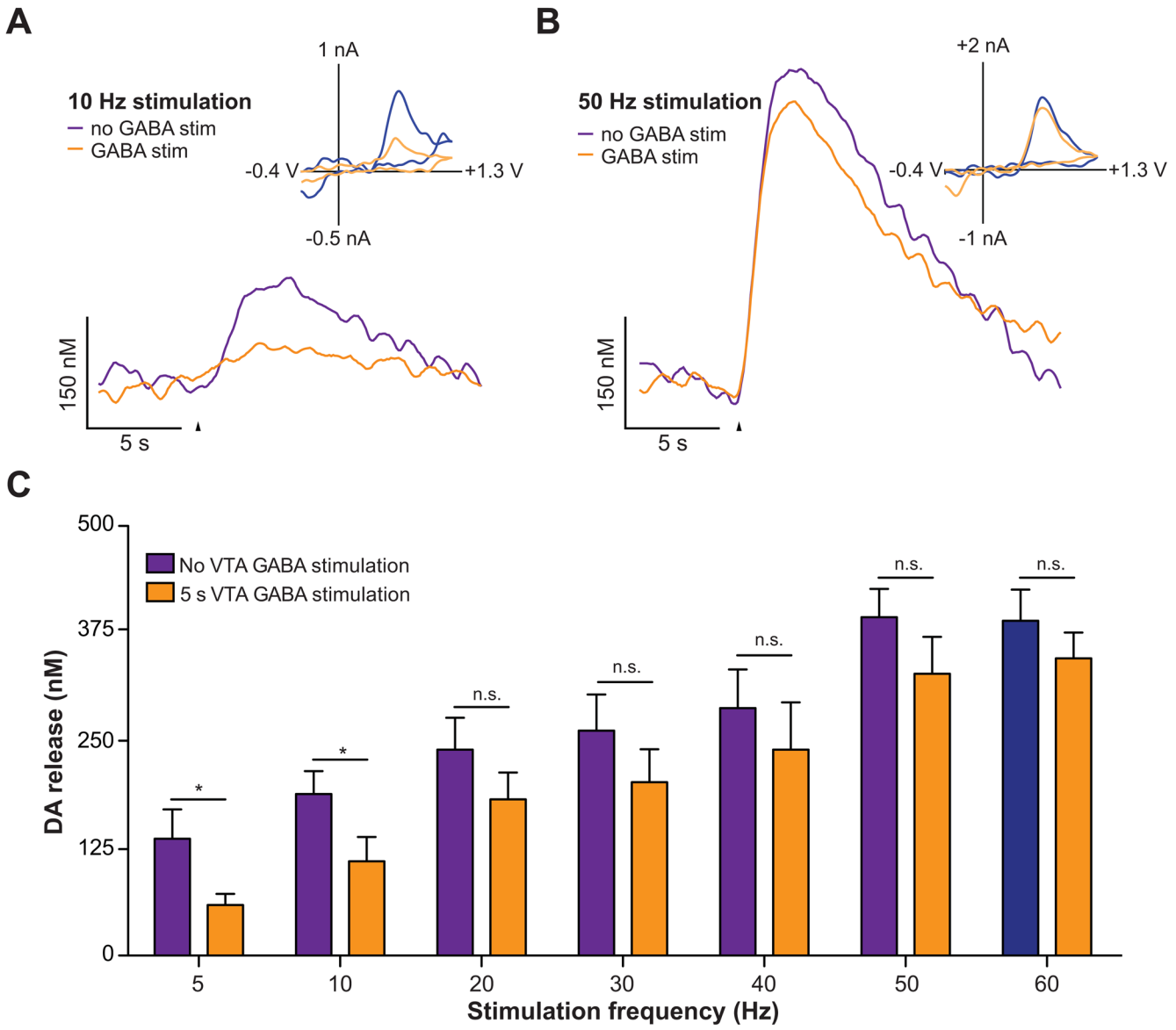


**Figure 5. Activation of VTA GABA neurons reduces electrically evoked DA release in the NAc**

(A) Voltammetric recordings indicated that activation of VTA GABA neurons reduces terminal DA release in the NAc induced by low frequency electrical stimulation of VTA. Representative concentration-time plots of electrically-evoked DA release measured in the NAc of anesthetized mice without (purple) and with (orange) optical stimulation of GABA neurons, which began 2.5 s prior to the VTA electrical stimulation and lasted for 2.5 s after. Arrowheads indicate the start of the electrical stimulation train. Inset shows background subtracted cyclic voltammograms, taken from the peaks of the signals, showing that the electrochemical signals were indicative of oxidized DA. (B) Voltammetric recordings with and without VTA GABA activation when the VTA is stimulated at a higher frequency. (C) Average data from all mice tested demonstrating frequency dependency of electrically-evoked DA release in the absence and presence of VTA GABA neuron activation (two-way ANOVA for a stimulation effect: $F(1,28) = 43.01$, $p = 0.0001$, n = 5 recording spots from n = 3 mice). Asterisks denote statistical significance (Bonferroni posttest, $p < 0.05$).